X-652-70-336
PREPRINT

NASA TM X-65350

THICKNESS OF IMPACT CRATER EJECTA ON THE LUNAR SURFACE

NICHOLAS M. SHORT
MICHAEL L. FORMAN

SEPTEMBER 1970

GSFC — GODDARD SPACE FLIGHT CENTER —
GREENBELT, MARYLAND

X-652-70-336
PREPRINT

THICKNESS OF IMPACT CRATER EJECTA ON THE LUNAR SURFACE

Nicholas M. Short and Michael L. Forman

Earth Observations Branch

Laboratory for Meteorology and Earth Sciences

September 1970

GODDARD SPACE FLIGHT CENTER

Greenbelt, Maryland 20771

THICKNESS OF IMPACT CRATER EJECTA ON THE LUNAR SURFACE

Nicholas M. Short and Michael L. Forman

Earth Observations Branch

Laboratory for Meteorology and Earth Sciences

ABSTRACT

Calculations based on improved models for impact cratering indicate an average thickness (if spread uniformly) of ejecta from craters and basins between 2 and 500 km diameters on the visible face of the Moon that ranges from 0.74 to 8.00 km (best estimate values between 1.36-2.39 km), depending on combinations of critical parameters utilized. These parameters include: (1) initial effective diameters of craters of excavation, (2) depth/diameter ratios between 0.05 and 0.35, (3) fractional enlargement of diameters by slumping (from zero to 50%), (4) efficiency of ejection, (5) frequency distribution of craters in the size range used, and (6) appropriate selection of circular structures as impact-generated. Chief uncertainty is the identification of those large basins definitely caused by impact; where mare-filled, the proper choice of diameter becomes critical. Contributions from mascon-related basins versus all roughly circular basins are treated separately. The general thinness of rubble cover ($\sim$ 1-20 meters) on some mare surfaces implies that most major craters were formed early in lunar history. An anorthositic lunar highlands (indicated by Apollo 11 results) should be covered to varying depths with ejecta derived largely from impact

basins cut into a pre-mare crust (anorthosite?) that was continuous around the lunar sphere. Ejecta from earlier (now covered or destroyed) craters plus unknown amounts of volcanic ash would add to the average thicknesses that can be calculated from observable impact craters.

CONTENTS

TABLES

THICKNESS OF IMPACT CRATER EJECTA ON THE LUNAR SURFACE

INTRODUCTION

Millions of circular structures ranging from fractions of a meter to hundreds of kilometers in diameter occur on the lunar surface. Most selenologists now agree that these structures are excavated cavities formed by explosions of considerable intensity. Both impact and volcanic processes can thus cause these craters. Current views accept both genetic types and recognize also a third, "hybrid" type consisting of an impact-generated crater which localizes and triggers volcanic responses such as interior lava filling, tumulis and squeeze-ups, cone venting, etc. Presence of shock metamorphism is cited by Short (1967, 1969) as evidence for the unique type of energy release and pressure wave action that separates an impact event from other crater-forming processes.

Both impacts and explosive volcanoes eject large volumes of fragmental materials. The total volume of ejecta from an impact crater supposedly matches the excavated volume of the primary or initial crater (Schroeter's rule; Pike, 1967). Thus, calculation of the sum of ejecta from all observable craters over a vast surface area should approximate the sum of excavation volumes of these same exposed craters. In contrast, the total volume of pyroclastic and lava-like materials expelled from volcanic structures will normally exceed any apparent excavated volumes because these fragmental materials are continuously

supplied through feeders from deeper zones within the Moon. Determination of the total volume of fragmental materials covering the Moon's surface, in terms of distributed thicknesses, can therefore serve as another test for the relative proportions of impact and volcanic craters.

On the Moon, the apparent absence of water precludes formation of layered aqueous sediments. Three processes not requiring water to produce layered units are: (1) volcanism involving lava and (anhydrous gas-supported) ash flows, (2) slumping and sliding of rubble during crater-wall collapse, mass-wasting, or tectonic movements, and (3) ballistic sedimentation associated with crater-forming impacts. In the top few kilometers of lunar crust, the first two processes probably make only minor contributions. Deposition of ejecta from impact craters appears to be the primary process that forms layered units above the Moon's hard crust. Many workers (e.g., Rinehart, 1959; Shoemaker, 1962; Gault et al. 1963; Roberts, 1966; Ross, 1968) have discussed the mechanisms by which this ejecta blanket is distributed and thickened. A singular characteristic of ballistic sedimentation, in distinction to most common sedimentary processes, is the extremely rapid rate of particle transportation and deposition. This gives rise to complexly interfingered and chaotically sorted units on surfaces subjected to intense, repetitious bombardment. Over time this leads to reworking and mixing of units so that well-defined, continuous layers representing individual events are gradually obscured. The usual criteria for recognizing specific stratigraphic boundaries and sequences and

for measuring thicknesses of distinguishable units obviously cannot be utilized in deciphering the nature and history of the lunar surface deposits. Nevertheless, a stratigraphic time-scale, based on classical superposition techniques applied to major surface units, was developed by the U. S. Geological Survey (Shoemaker, 1962; Shoemaker and Hackman, 1962; Wilhelms, 1967). Although these stratigraphic units have now been mapped over the entire front face (McCauley, 1967; Mutch, 1970), there are surprisingly few estimates of their thicknesses. Such estimates result from direct observations (telescope viewing; Lunar Orbiter); others were obtained by calculation from physical or statistical models not associated with particular areas.

An important goal in lunar exploration will be measurement of the relative proportions of "stratigraphic" thicknesses assigned to these fragmental impact ejecta deposits and to ash layers that together presumably cover much, if not all, of the lunar hardrock crust. Present indications, surveyed and summarized in this paper, favor a moonwide distribution of a sequence of extensive, more or less uniformly thick units of variably indurated impact ejecta that should contain significant amounts of shocked fragmental material. These units are piled up to average depths of 1 to 2 km except for thicker deposits where large basins have undergone considerable backfill.

The calculations are based on an improved model for impact cratering that determines ejecta volumes from craters of all sizes. Three varying depth-diameter functions are considered; observed crater diameters are adjusted

systematically for slumping. Crater parameters are taken from the System of Lunar Craters compiled by Arthur et al. (1963-1966) from telescope counts that classify over 17,000 circular structures between 1-400 km in diameter into groups according to size, stage of erosion (class), and location-age. Volume contributions from basins are treated as a special case. Thicknesses are then calculated as average values applicable to specific parts or the entire visible face of the Moon.

PREVIOUS STUDIES

Eggleton (1963) finds that the Apenninian series (comprised mainly of the Fra Mauro ejecta deposits from the Imbrium impact basin) in the Lansberg region varies in thickness from about 600 meters on the south to more than 1 km northward at the edge of Mare Imbrium. He begins with telescope mapping of hummocky deposits of this series and identification of older craters on a pre-Imbrian surface. Using the crater depth-diameter relationship given by Baldwin (1949), he calculates the thickness as equivalent to the depth of the smallest pre-Imbrian craters still visible beneath the Fra Mauro mantle. Offield (1970) suggests a thickness, based on topographic expression, for Fra Mauro units around the intended landing site of Apollo 13 to be 100-200 meters. McCauley (1964) cites thicknesses in the Orientale Basin west of the impact center amounting to 4, 1, and 0.1 km outward at distances of 300, 800, and 1200 km respectively. Units of the Procellarian system are estimated by Marshall (1963) to reach thicknesses of 1.1 km on average in the Lansberg region but up to 6 km

locally as fillings in partly covered to ghost craters. Carr (1965, 1966) assigns maximum thicknesses of 10 and 5 km to Procellarian materials in Mare Imbrium and Mare Serenitatis respectively.

The above estimates refer to regions of the Moon in which exposed deposits can be mapped as stratigraphic units and given formation or series names. Over most of the maria and perhaps much of the uplands as well, post-mare bombardments by particles ranging from micrometeorites to large meteorites have generated a loose, relatively thin and highly comminuted surficial layer termed the lunar regolith or soil. On the maria, this layer can be derived directly from immediately subjacent lava units and thus itself constitutes an incipient or early stage ejecta blanket; in most of the highlands terrain, the continually reworked "regolith" is assumed to develop mainly from underlying thick deposits identified as interfingered and mixed ejecta blankets built up largely from pre-mare cratering events. Oberbeck and Quaide (1967, 1968) have devised a method to estimate regolith thickness which relies on geometric form changes of fresh impact craters as a function of the ratio of crater diameter to the depth to more cohesive material beneath the fragmental surface layer. For a number of mare sites, including five at which Apollo landings are being considered (Quaide and Oberbeck, 1969), the median thickness of regolith was found to vary between 2 and 16 meters. Greater thicknesses can be expected in highlands terrain.

Salisbury and Smalley (1964) apply a simple cubic relation between crater radius and volume to calculate average thicknesses from observed primary

crater distributions. Their values are corrected for an assumed 26% pore space in the rubble volume. They obtain an even layer of rubble on the maria about 12.5 meters thick but point out that most ejecta materials concentrate in or near crater rims, leaving intercrater areas with an average thickness of only 0.63 meters. These workers find an even depth of 275 meters for rubble in the southern highlands and state that up to 1 km thicknesses of ejecta debris occur along the south edge of Mare Imbrium near the Apennine Mountains. They also note that increasing buildup of rubble layers progressively armors the surface against further destruction of bedrock by later cratering, particularly from secondary impacts.

Theoretical treatments using stochastic methods to estimate lunar ejecta thicknesses have recently been presented by Gault (1970), Marcus (1970) and Lindsay (1970). Gault starts with production rates for craters below any limiting size, based on size-frequency distributions derived from meteorite influx rates. Effects of equilibrium and saturation conditions on a surface enter into his model. As examples of typical results, Gault uses the Shoemaker-Whipple flux values to calculate an average depth of 94 meters in 10^9 years for ejecta accumulated at the equilibrium state from all craters up to 2.5 km diameter and an average depth of 6 meters for rubble produced on the surface at Sinus Medii over a period of 10^8 years when the Naumann-Hawkins flux rate is applied. Marcus presents a series of possible theoretical distributions of total ejecta blanket thicknesses built up from materials completely escaping

from paraboloidal craters. His calculations depend on excavations into initially plane surfaces by primary impact craters that follow an inverse power-law distribution. Lindsay obtains a fragment production-thickness buildup rate for primary impact debris using a function depending on the cumulative number of impacts per year for a range of expected meteorite flux masses, as modified from McCracken and Dubin (1963). He adjusts the accumulation rate to account for the shielding effect of thickening depositional units and for reworking of the fragmental layers. His results, however, are limited to estimates of regolith thicknesses in the maria and particularly at Apollo 11 and 12 sites.

BASIS FOR THE CALCULATIONS

Assumptions underlying the model for thickness calculations are outlined in Table 1 and discussed in this section.

1. Hardrock Crust

Most proposed origins of the Moon consider that it melted early in its history and then formed a solid crust. Possibly, this melting was confined to the outer regions of the lunar sphere. Apollo 11 rock sample investigations (Anderson et al., 1970; Short, 1970b; Wood et al., 1970) indicate the highlands may be anorthosites or anorthositic gabbros and could represent remnants of a primitive, once continuous crust.

Alternatively, an accretionary process without general melting has been proposed by advocates of a cold Moon history. This would lead to interfingered ejecta blankets extending below depths at which isolated or zonal melting provides the present mare lavas. Thus, rubble thicknesses of tens of kilometers may in

fact persist over most of the Moon, although compaction could produce coherent rock at shallower depths. The highlands, in this case, are remnants of unmelted accretions. This model, while plausible, will not be considered further.

2. Sequence of Events

The model assumes an initially uncratered melt-crust which is then immediately subjected to an extended period of intense bombardment by meteorites and comets. This results in build-up of a continuous (moon-wide) pre-mare ejecta blanket. At various times during this accumulation, some twenty large basins or central depressions are excavated by impact and become filled by lava flows that spill out beyond the inner basin rims onto lowlands to form the present maria. Following Hartmann (1966), the period of basin development is taken to be short relative to total lunar history and the interval of excavation and flooding occurred when the cometary-meteorite flux had declined appreciably. The radiogenic ages for Apollo 11 and 12 samples (Wasserburg, 1970) support this view; they show similar emplacement times of 3.6 and 3.4×10^9 years for lavas in Tranquillitatis and Oceanus Procellarum. Rubble from craters formed since mare filling is therefore expected to be meager compared with ejecta produced earlier. Thicknesses cited for the maria (Quaide and Oberbeck, 1969) tend to confirm this supposition.

3. General Crater Shape

From theoretical considerations, scaled impact experiments, and drilling at small terrestrial impact structures, it appears that the overall shape of an

impact crater is approximated by some simple geometric form. Marcus (1970) assumes a paraboloid in calculating such crater parameters as rim height and volume of displaced mass. Bjork (1962) uses this figure to describe earlier crater growth stages but his final crater follows a more bowl-shaped outline. A similar shape, involving a widened, nearly flat interior floor, was used by Pike (1967) to calculate the true crater volume. Oberbeck and Quaide (1967) consider final shape to depend on relative thicknesses and strengths of layers in the target medium. Pohn and Offield (1969) review various morphological types found among lunar craters and relate these both to genetic and to age factors; thus a given crater can pass through a series of shapes as it is worn down and/or buried by depositional processes.

No single geometric form fits all shapes expected from craters in rock or rock debris targets. In this paper, the spherical segment (Figure 1) is adopted as the form best approximating the boundary of a crater or basin of excavation (Short, 1970a). In volume calculations, a defines the initial (pre-slump) radius and h becomes the vertical depth from the point of impact (epicenter) to the central base of the excavated crater. As the diameter increases, the depth h of this segment decreases to account for the observation that larger craters produce correspondingly shallower indentations into their target materials. The total excavated volume is represented by the material lying between the original target surface and the spherical segment which outlines the boundary between the base of fallback ejecta and the underlying rupture zone. The final

crater profile shows two departures from this simple model: (1) the additional crater surface associated with the inner wall of an upraised rim, and (2) the new boundary between ejecta and rupture zone defined by the limits of slumping. Neither factor directly determines the volume of displaced (ejected) mass but both help to establish volumes of observed (final) apparent and true craters.

4. Depth and Diameter Variations

Baldwin (1949), Gault et al. (1968) and others have demonstrated that the maximum depth below the original surface at the impact epicenter to which excavation reaches will vary as a function of the effective crater diameter. Small craters excavate more deeply with respect to diameter than do successively larger ones. The fitted curve of explosion crater data given by Baldwin (1949, p. 131-133) can be extrapolated to a depth-diameter ratio of 0.2 for 1 km craters and 0.022 for a 500 km crater. Experimental impact studies show that differences in target strength, boundary conditions, etc. will cause some variation in this ratio for a given energy release.

Studies of small terrestrial impact structures (Short, 1970a, p. 637-638), indicate that simple craters (less than 3-5 km wide; no central peak) have depth (h) to diameter (d) ratios of about 1:3. Two values of h/d at 0.35 and 0.30 are selected for craters of 1 km widths. Larger terrestrial craters appear to be shallower, despite lack of quantitative confirmation by deep drilling. Three values of h/d at 0.20, 0.10, and 0.05 accordingly are chosen for 500 km craters. Intermediate h/d values can be taken from curves plotted from these end member values.

Experimental cratering studies (Gault et al., 1968) and investigations at several terrestrial impact structures (Dence, 1970; Short, 1970a) have shown the importance of slumping in which wedges of steep crater walls slip downward along shear surfaces in the rupture zone beneath the initial crater of excavation (Figure 1). Slumping apparently occurs almost immediately after crater excavation. Inward movements are nearly uniform around the entire lip of the crater. The degree to which the crater is enlarged is a function of the initial size of the excavation. Generally, smaller craters increase in diameter by 10-20% (e.g., West Hawk Lake in Canada; Short, 1970a). This is sufficient to backfill the central depression to depths that account for 25-50% or more of the original volume of excavation.

Most larger lunar craters appear to have slumped extensively to form a series of nested terraces. The estimated increases in diameter of 20-30% may even be low if inner terraces have slid into the central depression and now are hidden under lava or rubble covering the crater floor.

Extrapolation of the apparent increase in observed slump diameters from 10% for small craters through 20% for those of 50-100 km widths would result in values approaching 40-50% for 500 km basins of excavation. There is no clear evidence from lunar observations that terrace-forming slumps reach this magnitude, although J. F. McCauley (pers. comm., 1970) contends that slumping in the inner basin may be so extensive as to largely infill it prior to subsequent covering by lavas. However, the multiple ring structure of most lunar basins

may represent tilted annular blocks produced by inward slip movements similar to gravity slide faulting in terrestrial tectonism. This gives rise to a characteristic circumferential scarp and valley topography. The enlargement of circular basins by formation of outer rings can exceed 50% and may approach 100% of the original diameter. The innermost ring is rarely exposed to view as it is generally submerged beneath the lavas.

5. Energy Partition

Gault and Heitowit (1963) show that up to 80% of the kinetic energy of impact is expended in comminution of rock and throwout of ejecta. More than 90% of the displaced target volume is removed from the initial crater of excavation (Gault, pers. comm. 1969). Most ejecta particles leave the excavated region along low angle trajectories (Shoemaker, 1962; Gault et al., 1968). Studies of contained nuclear explosions (Short, 1966) indicate that only a few percent of the rock medium is directly converted to melt and vapor phases. On the Moon, less than 0.5% of the target medium, mainly the fraction subjected to intense shock pressures, receives ejecta velocities sufficient to escape the lunar gravitational field.

6. Thickness Distributions

The bulk of ejecta from an impact crater deposits in an apron or blanket distributed circumferentially around the crater rim (Shoemaker, 1962; Roberts, 1968; Marcus, 1970). Maximum deposition occurs just beyond the inner rim and decreases outward to an immeasurable minimum at distances ranging from

two to four crater radii with increasing crater size. Ejecta blanket volume is, according to Schroeter's rule (Pike, 1967), just equal to the volume of the crater excavation (neglecting possible compaction effects). On an extended, heavily cratered surface, repeated cratering redistributes ejecta deposits around individual rims into more uniformly thick and continuous layers as saturation and equilibrium conditions are reached (Oberbeck and Quaide, 1968; Gault, 1970). In these mature to old blanket deposits, departures from uniformity are associated primarily with proximity of any cratered area to large basins of excavation or to young, large craters (Tycho).

Thickness averages reported in this paper are calculated by summing up the total ejecta volumes and dividing by the surface areas assigned to the terrains considered. This averaging assumes that, given time, all ejecta is redistributed uniformly over the front side of the Moon provided that no further large craters or basins are added to impress into the hardrock surface beneath the blankets. In principle, however, a generalized picture of thickness variations in ejecta blankets can be reconstructed using the observed locations of large basins and craters to estimate departures from uniformity (p. 30).

7. Lunar Farside Contributions

Rays emanating from certain larger fresh craters extend outward many radii. Several associated with Tycho appear to pass completely around great circles on the lunar sphere (Chapman, 1969). The volume involved in these rays is small compared with the total ejecta in blanket deposits as only a very small

fraction of ejecta particles receive the high velocities and low trajectory angles suited to ray formation.

These rays, however, imply that some material ejected from larger craters and basins on the lunar frontside must have been deposited on the backside. Conversely, some backside-derived ejecta will cross over to areas on the frontside, especially near the limbs. Owing to lack of published crater counts for the Moon's farside as seen in Orbiter photographs, ejecta contributions from these craters are not considered in determining the thickness averages. Taking the Moon as a whole, contributions from the front and backsides are assumed to average out as equivalent. One exception is allowed for contributions from several basins situated near the limbs, as discussed on page 25.

8. Pre-mare Cratering

The present distribution of craters on the highlands is chosen as the best estimate of crater densities appropriate to a once-continuous pre-mare crust. In the University of Arizona Catalog (Arthur, 1963), all continental (terrae or highlands) craters regardless of age are assigned to this pre-mare group even though some class 1 and 2 craters may be post-mare in age.

In order to determine the pre-mare crater distribution beneath the present maria, the average volume of ejecta per unit area for the visible highlands is obtained by dividing the total volume from all continental craters by the area of exposed highlands (12.623×10^6 km^2; this value was suggested from planimetry results reported by Stewart-Alexander and Howard, 1970 and also Stewart-Alexander,

pers. comm., 1970). This unit value could then be converted to the total volume emanating from the sub-mare surface by multiplying by the total area now covered by maria. However, an alternate scheme for calculating thickness averages which included the pre-mare contributions from the areas now covered by maria is discussed on page 25.

9. Corrections for Crater Size

It is generally believed that the maria are largely filled with lava flows covered by a thin veneer of impact-derived rubble (regolith). The cumulative thicknesses of these flows have not been directly measured but various estimates range from less than 1 kilometer to 30 or more kilometers (page 33). The lavas presumably were extruded over the rubble that fills both the inner basins of excavation within the circular maria and any ejecta blankets surrounding these basins. Oceanus Procellarum and similar irregularly-shaped maria are treated as buried lowlands without underlying basin excavations.

In the maria, smaller craters will be contained almost entirely within the lava flows and will thus contribute mostly new crystalline rock material to the ejecta deposits. As crater diameters increase, the depths of crater penetration will also become greater until the crater bottoms pass into the older underlying rubble. From geometric considerations, the total volume of ejecta remains less than 50% of its final amount until a growing crater has expanded to 0.8 of its final depth h. Arbitrarily, when a crater is large enough for more than one-half of its volume of excavation to come from the buried rubble beneath the lavas,

it will not be included in the volume calculations because its contribution will then consist mainly of reworked ejecta deposits previously accounted for in the volume totals.

Owing to the uncertainty in specifying lava thicknesses, only a single case is considered. Thus, an average lava flow thickness of 5 km is chosen as representative of typical mare values. A crater that is 31 km in diameter is considered to have an h/d ratio of 0.2, so that a final penetration to about 6.3 km below the impact point will result. At 0.8th of this value, just 50% of the excavated volume will come from the interval between the surface and a 5 km depth. Craters larger than about 31 km will begin to excavate significant amounts of buried rubble from beneath the 5 km limit placed on lava thickness. These craters are therefore rejected as major contributors of new ejecta material to the lunar surface deposits.

Similar reasoning applies to the somewhat different situation on the highlands. Preliminary calculations showed that the ejecta blanket on the terrae would most likely be between 1 and 2.5 km thick. For an h/d of 0.2, excavation from a 15 km wide crater would extend to 3 km below the existing surface at impact. Using the 0.8 criterion, younger craters smaller than 15 km would derive most of their ejecta from the upper 2.4 km, or close to the higher value for the estimated thickness of the blanket. Adopting 2.4 km as the upper limit estimate of thickness for a "shielding" blanket, contributions from all C (continental) craters in classes 1 - 3 (many being post-mare) that are less than 15 km wide are treated

as reworked ejecta and hence are eliminated from the final volume calculations. Support for this view is found in the observation by Dodd et al., (1963), among others, that there is a relative rarity of ghost craters (most class 5 and some 4) smaller than 12 km in highlands terrain. This implies burial by an accumulating ejecta blanket at least 2 km thick.

In principle, as the blanket builds up, the limiting crater size below which shielding is ineffective should be constantly redetermined. However, crater ages, as defined by their classes, have not yet been correlated with thickness variations, so that this correction, while desirable, cannot be precisely applied. Recognizing also that many older craters now destroyed or buried have undoubtedly made contributions to the ejecta deposits, we have nevertheless confined the thickness determinations solely to the presently observable crater distributions.

Numerous erosion-deposition cycles can be postulated for most typical ejecta fragments. The distribution of any population of ejecta particles over time and space will be exceedingly complex, as described by Marcus (1970). Shock damage and other evidence in Apollo 11 microbreccia and soil samples indicate extensive turnover and reworking of the regolith overlying mare lavas owing to multiple impacts since cooling (Shoemaker et al., 1970). This overall effect of repeated burials and exposures must also characterize ejecta blankets on a larger scale. However, for simplicity, we treat the buildup of these deposits as a single- or first-cycle process in which ejecta volumes are equated exactly with volumes of exposed craters and inner basins of excavation.

10. Basins of Excavation

The frequency of craters larger than 500 km should fall somewhere near 0.1 per 10^6 km^2 on the lunar surface. Craters of this size will almost certainly be covered by mare lavas to varying extents and are normally referred to as basins. Craters larger than 250 km occur with a frequency of about 1 per 10^6 km^2; some of these are mare-free, others contain mare materials in their interiors, and a few may be completely submerged. Extrapolating to the total area of the Moon's frontside ($\sim 19.133 \times 10^6$ km^2), we can expect about 2 basins greater than 500 km in diameter and up to 20 craters and basins in the size range between 250-500 km.

The problem in verifying this distribution stems from the obscuring effects of the mare lavas. Only 4 craters larger than 250 km are listed in the University of Arizona catalog. However, most maria listed by Stewart-Alexander and Howard (1970) are associated with circular basins. Many such basins are identified as ringed structures by Hartmann and Kuiper (1962). Lunar specialists disagree as to exact dimensions of these basins but measurements normally are given as averages of the somewhat variable inner ring diameters. Diameters appearing in Table 5 are composited from Hartmann and Kuiper (1962), Kaula (1969), and Stewart-Alexander and Howard (1970). This gives one basin (Imbrium) larger than 500 km and 12 lying between 250-500 km. The latter total 16 when the 4 mare-deficient craters are added. These actual numbers of larger crater-basin structures agree reasonably well with the predicted numbers.

The surface area enclosed by these inner basins amounts to 1.79×10^6 km^2 or 27.3% of the total area (6.55×10^6 km^2) occupied by maria on the frontside. Compared with the total area of the frontside, these structures comprise $\frac{1.79 \times 10^6}{19.13 \times 10^6} \times 100 = 9.35\%$ of the visible face.

Well-defined rings are discernible within only 10 of the 20 more or less equidimensional named maria on the near side (Hartmann and Kuiper, 1962). Several large, nearly equant maria, such as Fecunditatis and Nubium, lack distinguishable ring structures, possibly because of isostatic adjustments and/or more extensive inundation by lavas.

Kaula (1969), Wise and Yates (1970) and others hold that basins co-associated with mascons most probably originated by impact. This implies that mascon-free circular basins may not be impact-generated. The question remains unsettled.

Therefore, two sets of calculations of contributions from these large structures are presented (Table 5). First, computations applied to all circular basins, with and without rings, are carried out. Second, only mascon basins are included in the volume summations. Because very large impact structures tend to be shallow, only the h/d function for the 0.30-0.05 limits is employed in these calculations. Inasmuch as slumping may be minimal within such shallow basins (being accommodated instead by ring structure development), just two slump conditions are considered: (1) no slumping and (2) slumping according to the 0.9-0.7 function.

11. Conversion of Volume to Thickness

Because all excavated volumes are assumed to spread uniformly across the lunar frontside, the total derived from both basins of excavation and post-mare cratering can be converted to average thicknesses through division by the area of the front face. However, two special cases require added explanation.

First, calculation of ejecta volumes from those hidden or destroyed craters now overlain by mare lavas must be determined by estimating pre-mare cratering contributions in similar areas on the highlands; thicknesses are then obtained by either of the two methods discussed in point 8. Second, to estimate the total thickness of ejecta remaining on the maria from all post-mare cratering, the accumulated volumes of all pM craters are divided by the combined areas assigned to all maria; contributions from neighboring highlands will constitute only a small fraction of this volume if terrae material is eventually shown to be dominantly anorthositic (King et al., 1970).

12. Porosity Corrections

Terrestrial impact structures contain generally tight and well-cemented fallback rubble. Both compaction and post-impact chemical changes consolidate the in-crater breccias and reduce bulk densities by granulating larger fragments and filling in pores.

Bulking of fragments within the collapsed chimney materials that fill cavities formed by contained nuclear explosions can increase total void porosity by 35% or more (Boardman et al., 1964); similar values apply to nuclear explosion

crater deposits. Initial porosities in ejecta falling beyond the rim experience smaller net reductions because of lesser load compaction under the thinner deposits.

Lunar ejecta deposits should behave similarly. The thin unconsolidated regoliths show densities of 1.5-1.7 g/cc (Costes et al., 1970) which indicate high initial porosities (greater than 50%) for fragmental materials of basaltic composition. Cementation of this material by fluid-carried substances has not yet been demonstrated as a lunar process. Microbreccias are derived by shock-lithification of the regolith (Short, 1970b) and perhaps other processes.

Without water and suitable cementing volatiles, thick deposits of lunar ejecta probably consolidate mainly by mechanical grinding and fracturing to produce smaller average sizes and better sorting, followed by improved cohesion through grain interlocking and electrostatic forces, and influenced by shock-wave compaction related to multiple impact events. As ejecta thicknesses build up, the lower layers are less likely to be disrupted by most events; porosity in these layers will steadily decrease as more overburden is added.

Until bulking and compaction changes in the lunar ejecta deposits are known, no corrections for porosity effects can be attempted. Ejecta thicknesses given in this paper are based on a zero porosity packing function. In reality, poorly sorted rubble in ejecta deposits of 1-2 km thicknesses should, in lunar gravity, have average porosities between 10-20% compared with only a few percent for their parent crystalline lavas or crustal rocks.

13. Isostatic Effects

Scott (1967) and Wedekind et al. (1970) indicate that lunar crater shapes - and hence volumes - change over time by rim collapse and uplift in the central depression in response to isostatic adjustments. Such long-term changes, especially effective in modifying larger craters and basins, will have no direct bearing on the amounts of ejecta produced. However, they can lead to errors in selecting appropriate crater diameters or in assigning relative ages to given circular structures.

CALCULATIONAL PROCEDURES

The sequence for calculating crater volume and ejecta blanket thicknesses, considering the assumptions previously discussed, is outlined in Table 2. Calculations using crater data extracted from a magnetic tape version of the University of Arizona catalog were carried out entirely by computer. Calculations involving only the 19 basin structures identified by Hartmann and Kuiper (1962) and others were made "by hand" using volume-diameter curves generated from the computer program.

The first step involves tabulation of crater frequencies arranged in 1 km increments for 6 combinations of classes and ages. The different groupings are used later in determining categories of contributors to the ejecta volumes. For convenience, craters distributed along continent-mare boundaries (MC types) are assigned to the highlands.

For any observed crater diameter, there will be several adjusted diameters, depending on which slumping function is picked, equal to or less than the final

(observed) one. Once selected, each adjusted diameter (for the initial crater of excavation) defines the appropriate value of h on the depth-diameter curve based on observed diameters.

The computer program automatically derives correct values for a and h for each of twelve combinations specified from the four slumping and three h/d functions. Volumes computed for increments in crater diameters at 1 km intervals are printed out in tabular form. These volumes are used to construct the volume-observed diameter plots shown in Figure 2.

The frequency of observed craters in every 1 km increment within each class-age grouping is mated with its corresponding size category for each of the 12 combinations. For basins of excavation beneath the maria, only combinations IA and IIIA were used in thickness calculations.

SUMMARY OF CALCULATED THICKNESSES

Table 3 summarizes volume calculations based on mating each of the six class-age groups with each of the twelve slump-h/d combinations. Average thicknesses derived from these values are recorded in two sets of three columns: the first set applies to all craters in the 2-500 km range whereas the second set removes contributions from craters above or below certain limits (point 9). For ejecta allowed to spread over the entire front face, column 1 entries in each set are obtained by dividing with the frontside surface area. Columns 2 and 3 apply to ejecta assumed to remain completely within the terrae and maria respectively.

Effects of removing contributions from craters greater than 31 km on the maria are computed by subtracting the volume values for all >31 km iterations from the total for group b combinations. Adjusted thicknesses are at least 60% less than those in equivalent columns in the first set. Thus, the relatively few large craters imposed on the mare lavas account for about 1/3 of the total ejecta. But, the absolute amounts of ejecta involved in post-mare cratering are quite small ($\sim 0.5\%$) compared with the total from all sources. Contributions from craters smaller than 15 km on the highlands are removed by subtracting volume values for all <15 km iterations from totals for group c. In contrast to the case for large mare craters, elimination of smaller, generally younger craters on the terrae (classes 1-3 are assumed to be mostly post-mare; classes 4 and 5 are considered residuals from initial cratering of the crust) changes the total volume or thickness of ejecta derived from highlands-type terrain by only 0.5-1.0%. Note also that post-mare cratering near continental margins (pMc in group e) adds only about 1-3% more ejecta to the totals for the class 1-3 populations represented by group c.

Ejecta thicknesses within the highlands are estimated by adding the volumes from adjusted group c results (column 2 in second set), which compensate for removal of <15 km diameter values, to volumes from group d and dividing by 12.62×10^6 km. Recalculated thicknesses representing post-mare contributions to the entire lunar frontside and to the mare alone are determined from the adjusted volume values under columns 1 and 3 respectively.

An alternate way of calculating the highlands contribution involves selection of a portion of the southern highlands as the best example of the ancient cratered crust. Thus, a region around the crater Abenezra lying within a rectangular loop bounded by direction-cosine coordinates ξ , η (University of Arizona catalog): +0.05, -0.18 → +0.25, -0.18 → +0.25, -0.50 → +0.40, -0.50 → +0.40, -0.75 → +0.05, -0.75 → +0.05, -0.18, approximately coincides with a part of the highlands nearly free of ejecta from major circular basins (p. 32). Only pure continental craters (all C, no CM) occur within this region. A computer run restricted to these selenographic coordinates determined the volumes of ejecta derived from groups c and d combined (equals group a in this case), without the trivial correction for contributions from <15 km craters. Assuming all ejecta remains in this region, the thickness total is obtained by dividing by its surface area of 1.014×10^6 km^2. Results are recorded in Table 4. Thicknesses characteristic of this region are about 10% less than those obtained for the highlands as a whole, which includes additions from the aMC craters.

Volume calculations for circular basins, using only combinations IA and IIIA, appear in Table 5. Thicknesses are derived by dividing the sum of volumes of all listed basins by the area 19.133×10^6 km^2. However, contributions from Mare Orientale were reduced by 2/3 and from Mare Australe by 1/2 to account for their proximity to the lunar disc limbs (point 7). A second summation of average thicknesses was produced by using only those volumes associated with basins underlain by mascons (point 10).

Wilhelms and McCauley of the U.S. Geological Survey Astrogeology Branch have presented arguments (pers. commun., 1970) for the existence of two additional large basins that are now mostly covered by mare lavas. The one centering around Copernicus is about 400 km in diameter; the other, located in the southern part of Oceanus Procellarum, is approximately 350 km wide. These basins would contribute, respectively, 0.104 and 0.073 km for Case I and 0.034 and 0.017 km for Case III to the average thickness of ejecta on the lunar surface derived from all basins. These values are not, however, added to the totals included in Table 5 inasmuch as the two new basins are not yet generally accepted as real lunar features.

Ejecta thickness values for either Case I or III can be added to any combination of slump and depth diameter values for thicknesses from either highlands model and from pM contributions by the >31 km diameter mare craters to give a grand total of 96 estimates (the product of the 12 combinations applied to craters times the two combinations of I and III for slumping in the basins times the results for the two groups of basins times the values for the two highlands models) of average ejecta thicknesses on the lunar front face. Many results are less likely than others and some are even improbable. Thus, conditions of no slump and maximum depths of excavation (h/d = 0.35-0.20) do not fit observations at terrestrial craters in hardrock and presumably would not apply to lunar craters in similar materials. Again, some impact-generated basins may not have detectable

mascons. However, the 96 estimates are expected to bracket the ranges of thicknesses originating from observed crater and basin distributions for all reasonable slump and depth variation cases.

From terrestrial studies, we consider that the IIIA combination (0.9-0.7 slump function and 0.30-0.05 h/d function) most closely approximates the behavior of impact craters for diameters appropriate to the Moon. This combination, together with the 8 highlands-basins slump-mascon conditions, defines the optimum or best estimate cases for average thickness of lunar ejecta. These thickness values are given in Table 6. We further believe that the best single value lies somewhere between 1.36 and 2.39 km (Cases 1 and 3, for either highlands model) assuming that mascons do not sufficiently identify circular basins and that large basins probably undergo moderate slumping that is less than predicted for somewhat smaller craters.

Conditions pertinent to maximum and minimum thickness estimates are reviewed in Table 7 along with final values for contributing thicknesses. The upper value is unrealistic as it ignores observations of actual slumping evident in larger craters. The lower value tends to overemphasize slumping and hence makes initial craters too small.

This table also includes a series of thickness values (in meters) (Case 3) extracted from Table 3 in which post-mare crater ejecta is allowed to remain solely within the maria. One special case, F, read from the tabulated computer data, gives a value for any mare region where all ejecta comes from craters

smaller than 10 km. This low value typifies areas within the maria suggested as possible Apollo landing sites to take advantage of the sparsity of nearby larger craters and reduced crater densities. Values from B through F fall within the ranges determined by Oberbeck and Quaide (1968) for the regolith at various mare localities. This close agreement supports the basic approach in estimating thicknesses as presented in this paper.

DISCUSSION OF RESULTS

It is clearly evident from the calculations that the mare-free regions of the Moon are presently covered by ejecta deposits to an average depth of at least 1 km. In places on the terrae this depth may exceed 2.4 km depending on the size and proximity of the closest major impact basin. Thicknesses comparable to the minimum assigned to the highlands (0.9–1.0 km) should have pre-existed in regions now covered by mare lavas. These sub-mare blanket deposits are still preserved in the lowlands except in those areas presently occupied by the inner basins. Pyroclastic ash beds and nues-ardentes-type units, if produced in quantity from lunar volcanism, could add significant volumes of material to the total of fragmental debris assumed to originate from impact processes alone.

The bulk of the impact ejecta deposits are derived from the larger craters and basins. Thus, all basins (i.e., with and without mascons) contribute from 37 to 50% of the ejecta (best estimate cases 1 and 3, Table 6) even though they comprise only 9.3% of the area on the Moon's visible side. When craters smaller

than 15 km are removed from the continental deposits, the net decrease in volume or thickness is insignificantly small. Again, mare craters below 30 km widths contribute only about 1/2 and those less than 10 km about 1/10th to the total ejecta produced from mare lava targets that stays exclusively within the maria. Two viewpoints are therefore supported: first, those millions of older and smaller craters that formed in hardrock add only small amounts to the ejecta total; second, shielding by growing rubble deposits has little effect on the overall accumulated thickness of such deposits in the terrae inasmuch as the larger structures will cut through any ejecta mantle to tap underlying bedrock as the source of most new throwout material.

The very low volumes and thicknesses associated with post-mare cratering is surprising. Various workers have noted that the crater population on the maria is roughly 1/10 to 1/30th that observed on the uplands. The University of Arizona catalog data indicates that there are only 1547 post-mare craters greater than 2 km wide in a total of 17,154 listed for all categories. The mare population has a density of $1.547 \times 10^3 \div 6.55 \times 10^6 = 0.236$ craters per 1000 km^2 whereas the terrae craters have a density of $15.607 \times 10^3 \div 12.62 \times 10^6 = 1.236$ craters per 1000 km^2 or a factor of 5 more frequent (without size differentiation). The thickness of post-mare ejecta deposits ($\cong$ regolith) residing on the maria, using the best estimate conditions (IIIA) is, for all craters, 17.8 meters compared with a value of at least 1,358 meters (Table 6, Case 1-I) for the average over the entire front face; this is slightly greater than 1% of the total. This deficiency of

materials reflects two critical factors; first, most mare craters are relatively small (1374 are under 10 km wide) and, second, the meteorite-comet flux density may have greatly diminished by the time craters began to form on the mare lavas (Hartmann, 1966).

The problem of constructing isopach maps showing actual thickness variations requires definition of a general model for the distribution of ejecta based on consideration of the ejecta deposits in and around large craters and circular basins. Shoemaker (1962) shows that the ejecta blanket (mainly missile ejecta and base surge deposits in Roberts' [1968] terminology) extends out to about two crater radii for small (1 km range) craters and to about three crater radii for craters of Copernicus size (~100 km). The ejecta blanket around the Imbrium basin can be traced to at least 1200 km (Eggleton, 1963) or about four crater radii. It appears then that the relative width of the ejecta blanket increases with increasing crater size.

A simplified distribution of ejecta around each basin can be specified by assuming that the average width of ejecta blankets surrounding the basins listed in Table 5 is 3.5 times the inner basin radius. The outer limits of these blankets with respect to the inner ring outline are drawn on Figure 3. This diagram shows that most of the Moon's front face is covered by one or more basin-generated ejecta deposits. In some regions (e.g., NE quadrant) three or more separate blankets, from different basins, are superimposed. Only an area extending south and west of Oceanus Procellarum and another in the southern

highlands seem relatively free of deposits contributed from the basins. This highlands area contains the region used in setting up a second model for calculating thicknesses of the terrae deposits (p. 25).

Terrestrial ejecta deposits tend to build up to depths that decrease exponentially outward from the inner rim of a crater (Roberts, 1968; Marcus, 1970) so that most throwout materials accumulate in a circumferential zone between 1 and 2 crater radii outward. However, expressions such as that given by Carlson and Jones (1965) apply to underground craters in which much of the ejected material is expelled along high angle trajectories and hence falls near the crater rim; atmospheric drag effects will also aid in concentrating lower angle ejecta in deposits just beyond the rim.

In a lunar vacuum, impact ejecta that follows low angle trajectories will probably spread out in deposits that thin more or less uniformly at a constant rate away from the rim. In cross-section, this tapering off in thickness can be depicted as a wedge whose base is nearly flat and upper surface inclines away from a maximum height next to the crater edge. Support for this mode of decreasing thickness is gained by plotting a profile for the limited number of estimated thicknesses of the Fra Mauro ejecta blanket south of the Imbrium Basin (Eggleton, 1963; Offield, 1970).

Based on this model of thickness variations, and using the distribution of basin ejecta as shown in Figure 3, a highly generalized isopach map of composite ejecta units on the lunar frontside has been constructed (Figure 4). An initial (pre-basin)

average thickness of 1 km is chosen to represent highlands terrain over which basin ejecta is absent. Thicknesses of basin ejecta are allowed to vary linearly from a maximum at 1 r to zero at 3.5 r. Where deposits from several basins are overlapped, thicknesses at various points within the areas of mutual coverage have been added. Contours appropriate to these areas have been smoothed out.

The isopach plot shows that maximum thicknesses occur around Mare Tranquillitatis and diminish somewhat towards Mare Serenitatis and Mare Fecunditatis. On a spheroid, deposits in these regions would appear to be topographically higher than in many places on the highlands. Studies by Baldwin (1963) and Mills (1968) show that, on average, the highlands are up to 2 km higher than the mare-covered areas. The seeming paradox in elevation is resolved by assuming that the lowlands floors have been depressed by amounts equal to the thicknesses of these ejecta deposits and overlying lavas plus the amount of average relief between maria and terrae.

The thickness variations within large basins themselves owing to fallback, mass-wasting, slumping, and other contributing sources, are difficult to assess because mare lavas have obscured underlying intrabasin deposits. However, an estimate of the depth of fill by both rubble and lava cover within these basins can be gained by an analysis of the inner basin under Mare Imbrium as a specific example (Table 8).

A no slump condition probably better fits a basin as large as Imbrium than do slumping enlargements as much as 20%. The rim height is calculated from an equation given by Baldwin (1963). The parameter involving the greatest uncertainty is the amount of backfill, because of two opposing factors. First, minimal slumping prevents extensive refilling. Second, a greater fraction of ejecta from very large craters or basins will tend to fall back directly into the central depression. A backfill to 50% of the maximum depth h in a spherical segment-shaped Imbrium basin results in a volume of 1.68×10^6 km^3 consisting of contributions from a 5% slump enlargement and a 20% return of initially ejected material. This comprises 0.314 of the volume of excavation for the no slump case (step 3, A; Table 8), a proportion nearly identical to that calculated for the West Hawk Lake impact structure (Short, 1970a). This backfill depth requires 10.1 km of lava to raise the basin floor to a level of 5.1 km below the Apennines rim - part of one of the outer rings which probably attained an elevation similar to the original inner ring. If backfill exceeds 0.5 h, the thickness of lava will decrease as indicated.

As yet, no evidence for the actual depth of excavation and ratio of rubble to lava infill within the Imbrium basin has been obtained from lunar exploration. In making mascon calculations, Baldwin (1968) obtains 51 km as the maximum (central) depth of excavation for an Imbrium basin ringed by a 25 km high rim and suggest that later infilling, mainly by extrusion of high density lavas, caused the basin floor to sink further. Conel and Holstrom (1968) assume that Mare

Serenitatis (for a diameter nearly identical to the Imbrium value used in this paper) requires filling with lavas that piled up to 14 and 31 km maximum thicknesses for density contrasts of 1.1 and 0.5 respectively between target and mare materials in order to account for the theoretical gravity profile over a basin of this size. Wise and Yates (1969) obtain isostatic equilibrium in a structure typical of an Imbrium basin by assuming that a 30 km mantle plug (ρ = 3.3) outpours above the plug top. Wood et al., (1970) consider a large basin to be filled by intrusion of a fluidized higher density basaltic mantle material into the depression punched through a lunar crust of different composition. All of these models favor a deeper initial basin and greater thickness of lava fill than proposed in this paper but, apparently, the role of backfilling by slumping, fallback, etc., is neglected in each.

The thickness of ejecta immediately adjacent to the inner rim, as calculated from a wedge-shaped cross-section, is about 2 km. A thickness of 3 km results from using the Carlson-Jones equations (see Marcus, 1970). Both values are reasonable in light of the 1 km plus thickness reported by Marshall (1963) at a distance of 2 radii where the Carpathian and Apennine Mountains form the second ring.

For a basin of Imbrium dimensions, therefore, a central fill of 10-25 km maximum thickness prior to lava invasion will grade outward (with a discontinuity at the rim) rapidly to 2-3 km just beyond the rim and thereafter will diminish to hundreds of meters at distances of 3 to 4 radii. The sequence of events taking place in the vicinity of major basins is illustrated in Figure 5.

The Imbrium results suggest that, on average, a value equal to 3 percent of the diameter of the inner ring approximates the thickness of ejecta backfill within the basins and largest craters. Thicknesses calculated in this manner for the various inner ring basins are not shown as isopach contours in Figure 4 owing to space limitations.

If the basins were impressed on a once-continuous crust of highlands-like rocks, then both the fraction of basin ejecta now lying beneath the maria and that fraction which overlaps on to the terrae should be lithologically similar to ejecta derived directly from the exposed continental crust. These highlands are probably mantled with thick ejecta topped by a thinner regolith, both derived mainly from underlying anorthosite (point 1) or its variants. Shock-lithified fragments of a possible anorthosite rubble originating in the terrae are described by Short (1970c) from both Apollo 11 and 12 samples. Smaller post-mare craters that excavate most of their ejecta from near surface lavas will add minor amounts of basaltic materials to the highlands deposits; however, larger post-mare craters like Copernicus and Erastothenes will return mainly sub-mare rubble of crustal nature if emplaced at points where mare lavas are less than 5 km thick.

CONCLUSIONS

The fundamental fact emerging from interpretation of the data presented in this paper is that the surface of the Moon is covered continuously by a thick mantle of rubble derived mainly as ejecta from the myriads of craters impressed over

time on the lunar crust. Ballistic sedimentation, an extremely rare and volumetrically insignificant process on Earth, is the dominant factor that builds up and modifies the outermost layer on the Moon.

Terrestrial sediments are localized primarily by structural undulations in an active crust which bring about repeated invasions of the seas on to geosynclinal troughs, shelfs and cratons. The distribution of lunar ejecta, considered as a composite stratigraphic sequence, is broadly analogous to the spatial occurrence of sedimentary units which cover parts of the mid-American craton. Thus, on the Moon a generally uniform blanket of impact (and volcanic?) debris about 1 km thick covers most of the highlands and extends with increasing thickness into wide circular depressions that attain their maximum depths in the center. This can be compared (without any genetic similarity) to the relations in the central United States between the thin (1-2 km) marine sediments deposited on a crystalline basement and the thicker (4-6 km) fillings into depressions (e.g., Michigan and Illinois Basins) within this basement.

Although the usual sedimentary processes do not operate on the Moon, the average cumulative thickness produced by ballistic sedimentation alone represents a value which, from both a relative and absolute measure, exceeds that assigned to terrestrial sediments. Blatt (1970) calculates the mean sediment thickness in the Earth's crust (using the global rather than continental surface area) to be about 830 meters. This value is nearly equivalent to that computed for the lunar highlands but is about half that suggested as the best estimate of the average

applicable to the entire lunar surface. Thus, we reach the surprising conclusion that the thickness of sediment-like rubble of impact origin on the lunar surface presently is proportionately higher than that of sediments derived from the conventional terrestrial processes of continental erosion and marine deposition. However, much of the igneous-metamorphic crust of sialic composition is believed to result from processes that converted earlier-formed sediments into crystalline rocks. Therefore, the total thickness of sediments over geologic time may be notably greater than the amounts now existing in the Earth's crust.

Three other consequences of the analysis presented in this paper of the processes leading to thickness buildup warrant special mention:

(1) All previous plots of cumulative frequencies of craters as a function of size (diameter) have been based on observed diameters. If slumping has enlarged the initial craters of excavation by 10-30%, then in effect these earlier size distributions contain an inherent error. The curves will therefore need to be shifted towards smaller diameters for each frequency value. This will influence either the estimates of meteorite-comet fluxes over time or the mass-velocity relations assumed in calculating energies required to produce craters of any given size.

(2) Pike (1967) notes two discrepancies in the expected 1:1 correspondence between crater rim volume and the true crater volume defined by Schroeter's rule. Fresh, smaller craters have ratios between 0.4-0.8 whereas older, larger craters

have ratios that can exceed 1.0. Isostatic adjustments and floor-filling by lava are cited as explanations for the departures associated with larger craters. Explanations applied to the smaller craters are less convincing inasmuch as accurate calculations of rim volumes and, especially, of the depths of excavation needed to calculate true crater volumes cannot be made adequately from telescopic or Orbiter observations. Gault et al., (1968) show from experimental impact cratering that most target material ends up as ejecta that leaves the crater, so that Schroeter's rule should apply closely. Explosions craters, however, toss a greater proportion of the ejecta upward along high-angle trajectories, so that more material falls directly back into the crater and therefore lowers the rim: true crater volume ratio below 1.0. The low values of this ratio for the fresh, younger lunar craters would, at first glance, seem to favor an internal explosive origin inasmuch as impact craters should obey Schroeter's rule within the limits of observational errors. But, the excess of true crater volume, as reported by Pike from studies by Baldwin (1963) and Abrams (1966), may be a real effect. If so, it can be readily accounted for by slumping which would provide for a larger diameter (and hence greater true crater volume) and would also remove some of the innermost rim deposits.

(3) Pike (1967) further describes a break in the slope of the curve that plots the "interior relief" or "crater depth" R_i as a function of rim crest diameter D_r. This occurs within the diameter interval 10-20 km (at approximately a 15 km threshold value). Thus, craters larger than this value have shallower depths

relative to their diameters than do smaller craters. Pike considers this slope change to indicate modification by post-impact deformation (central peak and floor uplift; isostatic adjustment).

Although this explanation may be correct, another possibility can be advanced. Oberbeck and Quaide (1968) observe a flattening of crater floors, which can be expressed by a lower R_i/D_r ratio, for cases in which the relative thickness of surficial (regolithic) material is either less than $D_r/3.8$ or greater than $D_r/10$. Normal and concentric craters develop where the regolith is relatively thicker or thinner respectively for a given diameter; absolute thicknesses will diminish with decreasing crater size. For a very thick deposit (equating ejecta blankets with regoliths), a flat-floored crater of 15 km diameter will thus form if the upper layer is between 1.5 and 4.0 km in thickness (these thickness limits will reduce slightly when the diameter is adjusted for slumping).

The essence of our argument is this: On the highlands, we have arrived at average thickness values ranging from a minimum of 1.0 km to 1.5-2.5 km in areas closer to large basins. Craters smaller than about 10 km will be normal whereas those larger than 25-30 km will be concentric by analogy to examples depicted by Oberbeck and Quaide for regoliths on the maria. At a threshold size of 15 km, the true crater depth is about 1.5-2.0 km depending on the h/d curve used. Thus, at this diameter a developing crater of excavation within the ejecta blanket begins to penetrate well into the subjacent hard crust. Although Oberbeck and Quaide do not claim that formation of flat-floored craters would depend on the relative

strengths of the upper (ejecta blanket or regolith) and lower (crustal) layers, for large craters the presence of a more resistant hard rock layer beneath the weakly cohesive overlying layer might promote development of this particular morphology. This is supported by parameters determined from experimental nuclear explosion craters in different media (Nordyke, 1964): for a given scaled depth of burial normalized to 1 kiloton, craters in basalt are less wide and deep than those in alluvium.

(4) Pohn and Offield (1969) call attention to a general change in the (plan view) outline of lunar craters from essentially circular to more or less polygonal as craters become larger than about 20 km. Assuming that polygonality is controlled primarily by jointing (as illustrated by Meteor Crater, Arizona) in the lunar crust (lunar grid system), as some have proposed, then the same argument put forth in consequence 3 will also apply here. Thus, the rim and inner wall morphology of craters smaller than 15-20 km will be influenced mainly by the behavior of the fragmental debris within the ejecta blanket during both excavation and slumping stages. If a significant fraction of the lower crater is developed within a jointed, hardrock crust, as would be expected in craters bigger than 15-20 km in areas where the overlying blanket deposits are around 2-3 km thick, the effects of this jointing will be sufficient to modify and perhaps dominate the final shape of the craters that depart from circularity. Pohn and Offield further note that craters larger than about 40 km begin to lose their polygonal character and instead become constructed of a series of short, arcuate scallops that together can be

closely circumscribed by an outlining circle. This pattern presumably is related to slump scars associated with the concentric terracing that is observed in most large craters.

Indirectly then, the shifts in crater morphology from circular to polygonal and from normal to flat-bottomed at the size range between 15-20 km would seem to confirm the estimate of 1.0 to 2.5 km of ejecta rubble in areas now free of an overlying lava cover. It may be possible to verify or reject this conclusion by comparing systematic measurements of depth-diameter relationships, crater interior geometries, and rim outlines in selected parts of the terrae and maria. Fundamental differences in these morphological parameters as a function of crater diameter should be evident if the lowlands are covered, on average, with several kilometers of rubble deposits in contrast to a near-surface occurrence of thick (2-5 km) units of hardrock lavas over most of the mare lowlands.

Another supporting argument is given by Blodgett et al., (1970) from analyses of the types of landslides observed in large lunar craters. They conclude that the inner walls in Copernicus-size craters on the maria fail by sliding of wide blocks or terraces consisting of near-surface "bedrock" whereas downslope movements of walls in similar-sized highlands craters are more like "landslides" composed of thin slabs or slices. These landslides are consistent with behavior of materials having low shear strengths, from which they conclude that the terrae are covered by a "very deep layer of fragmental rock".

Seeger (1970) and others have claimed that both hardrock layers and fragmental debris are visible in the walls of some of the major craters observed in Lunar Orbiter photos. However, evidence for a high proportion of lava or crustal bedrock is limited and unconvincing. Slumping can disturb or destroy signs of bedrock layers in mare craters. Slump masses would bury the lower walls of both mare and highlands craters.

Finally, the hypothesis put forth in this paper - that the lunar surface is composed of a continuous mantle of impact-derived debris reaching thicknesses of 1-2.5 km - will be subjected to stringent tests during further exploration in the Apollo program. Thus, analysis of seismic signals from natural or induced moonquakes will aid in evaluating the kinds of material (and their thicknesses) making up the near-surface and subcrustal rocks. As the Apollo seismic network spreads to other landing sites, the possibility of determining thicknesses over large areas of the Moon will improve substantially. The "mystery" of the exceedingly long duration signals from spacecraft impacts on the lunar surface (Latham et al., 1970) may be resolved by assuming a model of several kilometers of lower velocity ejecta in a continuous blanket that is overlain by lava flows in the lowlands and underlain by hardrock crust in the highlands. Ultimately, on-site studies by trained astronaut observers, documented by extensive photography and sample collection, can best shed new light on the nature and occurrence of layered rocks - be they impact ejecta deposits, ash beds, lava flows, or multiple intrusions - on the Moon.

REFERENCES

Abrams, W. J., An investigation of Schroeter's rule, Astron. Contrib. Boston University, series 2, no. 42, 1966.

Anderson, A.T., A. V. Crewe, J. R. Goldsmith, P. B. Moore, J. C. Newton, E. J. Olsen, J. V. Smith, P. J. Wyllie, Petrologic History of Moon as suggested by petrography, mineralogy, and crystallography, Science, 167, 587-590, 1970.

Arthur, D. W. G., A. P. Agnieray, R. A. Horvath, C. A. Wood, and C. R. Chapman, The system of Lunar craters, Quadrants I-IV, Comm. Lunar & Planet. Lab., University of Arizona, 2, p. 71 (1963), 3, p. 1, 3, p. 61 (1964-1965), 5, p. 1 (1966).

Baldwin, R. B., The Face of the Moon, University of Chicago Press, Chicago, 1949.

Baldwin, R. B., The Measure of the Moon, University of Chicago Press, Chicago, 1963.

Baldwin, R. B., Lunar mascons - another interpretation, Science, 162, 1407-1408, 1968.

Bjork, R., Analysis of the formation of Meteor Crater, Arizona, J. Geophys. Res., 66, 3379-3387, 1962.

Blatt, H., Determination or mean sediment thickness in the crust: a sedimentologic method, Bull. Geol. Soc. Am., 81, 255-262, 1970.

Blodget, H. W., P. D. Lowman, Jr., and J. A. O'Keefe, Geologic analyses of selected Apollo 10 70 mm Lunar and terrestrial photographs, in press, 1970.

Boardman, C. R., D. D. Rabb, and R. D. McArthur, Responses of four rock mediums to contained nuclear explosions, J. Geophys. Res., 69, 3457-3469, 1964.

Carr, M. H., Geologic map of the Timocharis region of the Moon, U. S. Geol. Surv. Misc. Geol. Inv. Map I-462, 1965.

Carr, M. H., Geologic map of the Mare Serenitatis region of the Moon, U. S. Geol. Surv. Misc. Geol. Inv. Map I-489, 1966.

Chapman, D. R., Origin of Australasian tektites, 3rd Intern. Tektite Sympos., Corning, N. Y., April, 1969.

Conel, J. E. and G. B. Holstrom, Lunar mascons - a near-surface interpretation, Science, 162, 1403-1404, 1968.

Costes, N. C., W. D. Carrier, and R. F. Scott, Apollo 11 Soil Mechanics Investigations, Science, 167, 739-742, 1970.

Dence, M. R., Structure of the Brent crater, Ontario, Geol. Assoc. Canada Proc., in press, 1970.

Dodd, R. T., Jr., J. W. Salisbury, and V. G. Smalley, Crater frequency and the interpretation of lunar history, Icarus, 5, 399-405, 1963.

Eggleton, R. E., Thickness of the Apenninian Series in the Lansberg region of the Moon, in Astrogeol. Studies Ann. Prog. Rept., Aug. 1961-Aug. 1962, U.S. Geol. Surv. open file report, 19-31, 1963.

Gault, D. E., Saturation and equilibrium conditions for impact cratering on the lunar surface: criteria and implications, Radio Science, 273-291, 1970.

Gault, D. E., E. M. Shoemaker, and H. J. Moore, Spray ejected from the lunar surface by meteoroid impact, NASA Tech. Note D-1767, Washington, D. C., 1963.

Gault, D. E., and E. D. Heitowit, The partition of energy for hypervelocity impact craters formed in rock, Proc. Sixth Hypervelocity Impact. Sympos., Cleveland, 1963.

Gault, D. E., W. L. Quaide, and V. R. Oberbeck, Impact cratering and mechanics, Shock Metamorphism of Natural Material, (B. M. French & N. M. Short, edit.), Mono, 87-99, 1968.

Hartmann, W. K., Early lunar cratering, Icarus, 5, 406-418, 1966.

Hartmann, W. K. and G. P. Kuiper, Concentric structures around lunar basins, Comm. Lunar & Planet. Lab., University of Arizona, 1, 51-66, 1962.

Kaula, W. M., Interpretation of lunar mass concentrations, Phys. Earth Planet. Interiors, 2, 123-137, 1969.

King, E. A., Jr., M. F. Carman, and J. C. Butler, Mineralogy and petrology of coarse particulate material from lunar surface at Tranquillity Base, Science, 167, 650-652, 1970.

Latham, G. V., M. Ewing, F. Press, G. Sutton, J. Dorman, Y. Nakamura, N. Toksoz, R. Wiggins, J. Derr, and F. Duennebier, Passive seismic experiment, Apollo 11, Science, 167, 455-458, 1970.

Lindsay, J. F., A depositional model for post-mare debris on the lunar surface, J. Geol., in press, 1970.

Marcus, A. H., Distribution and covariance function of elevations on a cratered planetary surface, The Moon, 1, 1-41, 1970.

Marshall, C. H., Geologic map of the Letronne region of the Moon, U. S. Geol. Surv. Misc. Inv. Map I-385, 1963.

McCauley, J. F., The stratigraphy of the Mare Orientale region, Astrogeol. Studies Ann. Prog. Rept., Aug. 1962-July 1963, Pt. A, U. S. Geol. Surv. open file report, 86-98, 1964.

McCauley, J. F., The nature of the lunar surface as determined by systematic geologic mapping, Mantles of the Earth and Terrestrial Planets (S. K. Runcorn, edit.) Interscience, London, 431-460, 1967.

McCracken, C. W. and M. Dubin, Dust bombardment on the lunar surface, NASA Tech. Note D-2100, Washington, D. C., 1963.

Mills, G. A., Absolute coordinates of lunar features, Icarus, 8, 90-116, 1968.

Mutch, T. A., Geology of the Moon, Princeton University Press, 324 pp., 1970.

Nordyke, M. D., Cratering experience with chemical and nuclear explosives, in Third Plowshare Symposium Proc., U. S. Atom. Energy Comm. TID-7695, 51-74, 1964.

Oberbeck, V. R. and W. L. Quaide, Estimated thickness of a fragmental surface layer of Oceanus Procellarum, J. Geophys. Res., 72, 4697-4707, 1967.

Oberbeck, V. R. and W. L. Quaide, Genetic implications of lunar regolith thickness variations, Icarus, 9, 446-465, 1968.

Offield, T. W., Geologic map of part of the Fra Mauro region of the Moon - Apollo 13, U. S. Geol. Surv. Rept. Orb III S-23(25), 1970.

Pike, R. J., Schroeter's rule and the modification of lunar crater impact morphology, J. Geophys. Res., 72, 2099-2106, 1967.

Pohn, H. A. and T. W. Offield, Lunar crater morphology and relative age determination of lunar geologic units, U. S. Geol. Surv. Interagency Rept., Astrogeol. 13, 35pp, 1969.

Quaide, W. L. and V. R. Oberbeck, Thickness determinations of the lunar surface layer from lunar impact craters, J. Geophys. Res., 73, 5247-5270, 1968.

Quaide, W. L. and V. R. Oberbeck, Geology of the Apollo landing sites, Earth-Science Rev., 5, 255-278, 1969.

Rinehart, J. S., Meteorites and ballistics, in Selected Topics on Ballistics, Pergamon Press, New York, 1959.

Roberts, W. A., Shock - a process in extraterrestrial sedimentology, Icarus, 5, 459-477, 1966.

Roberts, W. A., Shock crater ejecta characteristics, Shock Metamorphism of Natural Materials (B. M. French & N. M. Short, edit.), Mono, 101-114, 1968.

Ross, H. P., A simplified mathematical model for lunar crater erosion, J. Geophys. Res., 73, 1343-54, 1968.

Salisbury, J. W. and V. G. Smalley, The lunar surface layer, in The Lunar Surface Layer: Materials and Characteristics, (J. W. Salisbury and P. E. Glaser, edit.), Academic Press, 411-444, 1964.

Scott, R. F., Viscous flow of craters, Icarus, 7, 139-148, 1967.

Seeger, C. R., A geological criterion applied to Lunar Orbiter V photographs, Modern Geol., 1968, 1, 203-210, 1970.

Shoemaker, E. M., Interpretation of lunar craters, in Physics and Astronomy of the Moon, (Z. Kopal, edit.), Academic Press, London, 283-359, 1962.

Shoemaker, E. M. and R. J. Hackman, Stratigraphic basis for a lunar time scale, in The Moon, (Z. Kopal & Z. K. Mikhailov, edit.), Academic Press, London, 289-300, 1962.

Shoemaker, E. M., M. H. Hait, G. A. Swann, E. L. Schleicher, D. H. Dahlem, G. G. Schaber, R. L. Sutton, Lunar regolith at Tranquillity base, Science, 167, 452-455, 1970.

Short, N. M., Effects of shock pressures from a nuclear explosion on mechanical and optical properties of granodiorite, J. Geophys. Res., 71, 1195-1215, 1966.

Short, N. M., A review of shock processes pertinent to fragmentation and lithification of the lunar terrain, in Interpretation of Lunar Probe Data, (J. Green, edit.), Sci. and Tech. Ser., Am. Astronautical Soc., 14, 17-60, 1967.

Short, N. M., Shock metamorphism of basalt, Modern Geol., 1, 81-95, 1969.

Short, N. M., Anatomy of a meteorite impact crater: West Hawk Lake, Manitoba, Canada, Bull. Geol. Soc. Am., 81, 609-648, 1970a.

Short, N. M., Evidence and implications of shock metamorphism in lunar samples, Science, 167, 673-675, 1970b.

Short, N. M., The nature of the Moon's surface: evidence from shock metamorphism in Apollo 11 and 12 samples, Icarus, in press, 1970c.

Stuart-Alexander, D. E. and K. A. Howard, Distribution of lunar maria and circular basins, Icarus, V. 12, No. 3, 1970.

Wasserburg, G. J., The Moon: Observations and conclusions from Apollo 11 and 12, invited paper, 51st Ann. Mtg., Amer. Geophys. Un., Washington, D. C., April, 1970.

Wedekind, J. A., D. E. Gault, and R. Greeley, Model studies of isostatic readjustments of large impact craters, (abst)., Trans. Amer. Geophys. Un., 51, p. 342, 1970.

Wilhelms, D. E., Summary of telescopic lunar stratigraphy, U. S. Geol. Surv., Astrogeologic studies, Ann. Prog. Rept., A, 237-305, 1966.

Wise, D. U. and M. T. Yates, Mascons as structural relief on a lunar "Moho", J. Geophys. Res., 75, 261-268, 1970.

Wood, J. A., J. S. Dickey, U. B. Marvin, and B. N. Powell, Lunar anorthosites, Science, 167, 602-604, 1970.

Table 1

Strategy and Assumptions

POINT

1. Initially, Moon completely enclosed by hard rock crust (anorthosite?).
2. Idealized general sequence of ejecta deposition:
   A. Cratering of entire hard rock surface (represented by highlands).
   B. Ringed basins (most sub-mare) formed during narrow span of lunar time, then filled with slump rubble and lava extrusions.
   C. Post-mare cratering: Contributions mainly from smaller craters on mare and larger craters (31km cutoff) on terrae.
3. Observed crater diameters may be greater than original diameters because of slumping enlargements: depth/diameter ratios vary with crater size.
4. Crater volumes for craters and basins of all sizes from the formula for a spherical segment: $V = \pi/6\ h(h^2 + 3a^2)$; a is initial radius and h is maximum depth of excavation.
5. All volume within crater of excavation converted to fragmental material, melt, & vapor: most ejecta is throwout: less than 0.5% escapes lunar gravity.
6. Schroeter's rule applies; all ejecta is assumed to redistribute uniformly over entire front side or in selected areas.
7. Contributions from back side just balanced by ejecta transported from front side to back.

Table 1 (continued)

POINT

8. Thicknesses calculated for present-day highlands serve to estimate thicknesses in pre-mare regions now occupied by basins and maria.

9. Contributions from craters larger than 31 km wide in the maria and smaller than 15 km wide in the highlands can be discarded from the final volume totals because they represent reworked materials; ejecta considered first-cycle only.

10. Basins of excavation (generally under mare cover) larger than 200 km are ringed: diameter is taken as that of inner ring (Hartmann & Kuiper, 1962) with or without slump increases; basins selected either (a) all ringed structures or (b) mascons only.

11. Average thickness of ejecta on front side calculated as:

    A. Total volume of pre-mare cratering on highlands 12.62×10^6 km^2 (area of exposed terrae), plus:

    B. Total volume of basins of excavation (all or mascons only) 19.13×10^6 km^2 (area of front side), assuming uniform spreading, plus:

    C. Total volume of pM (post-mare) craters 19.13×10^6 km^2; or, for thickness confined to maria alone 6.55×10^6 km^2 (area of all maria).

Table 1 (continued)

POINT	
12.	Reported thicknesses are based on zero porosity; bulking of ejecta increases actual thicknesses by estimated 25% or more, depending on compaction, etc.
13.	Possible modifying effects from lunar surface curvature, isostatic adjustments, etc. on volumes and observed diameters are not incorporated into the model or the calculations.

Table 2

Sequence of Calculation Steps (Generalized)

1. Data on magnetic tape containing lunar crater parameters from the U. of Arizona LPL Catalog (Arthur et al.) are read and restructured to format suited to computer programming.

2. Crater frequencies as functions of observed diameters from 2-400 km are summed from catalog data and arranged in tables at 1 km increments according to these class and age groupings:

   a) all classes; ages 1-5
   b) pM; 1-5
   c) C, aMC; 1-3
   d) C, aMC; 4-5
   e) C, aMC; pMC; 1-3
   f) aM; 1-5

3. Crater volumes are calculated from equation: $V = \pi/6\ h(h^2 + 3a^2)$, where a is the adjusted crater radius (km) determined by multiplying the observed crater diameter ($\div 2$) reported in the catalog by the following slumping factors: (I.) 1.0 (no slumping) for all diameters between 2-400 km; (II.) 0.9 (1 km) to 0.8 (400 km), with interpolated factors for diameters within this range; (III.) 0.9 - 0.7 for this range; and (IV.) 0.9 - 0.5 for this range; and where h is the crater depth (vertical interval between original surface at point of impact and base of crater of excavation) for the following assumed ratios of h/d: (A.) 0.30 (1 km) to 0.05 (400 km) and intermediate values as determined from a linear plot of these X, Y limits; (B.) 0.35 - 0.10 for this range; and (C.) 0.35 - 0.20 for this range, in

which each diameter d is the adjusted value for a specific slump condition. These combinations of adjusted a's and h's are thus calculated for each observed (index) diameter in 1 km increments from 2-400 km:

IA, IB, IC IIA, IIB, IIC IIIA, IIIB, IIIC IVA, IVB, IVC

4. The number of craters determined in step 2 for each 1 km diameter increment within class-age groupings a) thru f) is multiplied by each calculated volume for that size interval for every case set up in step 3 from IA thru IVC, providing 72 tables of volumes. For each crater frequency-volume table, cumulative volume sums are reported for every 10 km diameter increase and the total for the 400 km end point represents the contribution of all craters from 2-400 km for each set of class and age-slump radius $a - h/d_{adj}$ run.

5. The volumes of basins of excavation for observed or presumed ringed basins (most are mare-covered) are computed for the same h/d variations but only slumping factors I and III are used. Diameters selected are those given in Hartmann & Kuiper (1962), with several values modified from more recent estimations. The sums of these values are reported on two bases: (a) all ringed structures listed by Hartmann & Kuiper, and (b) only those basins with mascons.

6. The accumulated volumes for the different a_{adj} and h/d_{adj} combinations are divided by the following surface areas:

Table 2 (continued)

X) 19.133×10^6 km^2 for the entire front side of Moon

Y) 12.623×10^6 km^2 for area of exposed terrae (uplands)

Z) 6.550×10^6 km^2 for area of maria (34%) on front face

By applying one or more of these divisors to the six class-age groups as follows:

a) - X b) - X, Z c) - Y d) - Y e) - Y f) - X, Z

The contributions from the sub-mare basins of excavation are assumed to spread out over the entire front face and hence are divided by X.

7. Resulting thicknesses are summed in various combinations, according to reasoning presented for each individual case; generally, the total thickness for any given case will include contributions from c) + d) + b) + mare basins; special cases are discussed in the text.

Table 3

Summary of Thickness Calculation Data

No.	Slump	h/d	Group	Volume x 10^7 km^3	Thickness (km) 1	2	3	Adjusted Volume x 10^7 km^3	Adjusted Thickness (km) 2	3
1	I	A	a	3.019	1.689					
2	I	B	a	4.494	2.514					
3	I	C	a	6.959	3.894					
4	II	A	a	1.825	1.021					
5	II	B	a	2.653	1.484					
6	II	C	a	3.771	2.222					
7	III	A	a	1.423	0.796					
8	III	B	a	2.042	1.142					
9	III	C	a	2.999	1.678					
10	IV	A	a	0.797	0.446					
11	IV	B	a	1.113	0.623					

Table 3 (Continued)

No.	Slump	h/d	Group	Volume x 10^7 km^3	Thickness (km)			Adjusted Volume x 10^7 km^3	Adjusted Thickness (km)		
					1	2	3		1	2	3
12	IV	C	a	1.564	0.875						
13	I	A	b	0.0227	0.0130		0.0348	0.0072	0.0040		0.0111
14	I	B	b	0.0311	0.0170		0.0478	0.0094	0.0052		0.0145
15	I	C	b	0.0424	0.0240		0.0651	0.0114	0.0064		0.0175
16	II	A	b	0.0142	0.0080		0.0218	0.0047	0.0026		0.0072
17	II	B	b	0.0192	0.0110		0.0295	0.0061	0.0034		0.0094
18	II	C	b	0.0255	0.0140		0.0392	0.0073	0.0041		0.0113
19	III	A	b	0.0116	0.0065		0.0178	0.0041	0.0023		0.0063
20	III	B	b	0.0156	0.0087		0.0240	0.0053	0.0030		0.0087
21	III	C	b	0.0205	0.0110		0.0315	0.0063	0.0035		0.0097
22	IV	A	b	0.0075	0.0040		0.0115	0.0030	0.0017		0.0046
23	IV	B	b	0.0099	0.006		0.0152	0.0039	0.0022		0.0060

Table 3 (Continued)

No.	Slump	h/d	Group	Volume x 10^7 km^3	Thickness (km)			Volume x 10^7 km^3	Adjusted Thickness (km)		
					1	2	3		1	2	3
24	IV	C	b	0.0126	0.007		0.0194	0.0045	0.0025		0.0069
25	I	A	c	1.345	0.753	1.065		1.340	0.749	1.061	
26	I	B	c	1.977	1.106	1.566		1.970	1.110	1.561	
27	I	C	c	3.000	1.683	1.382		3.000	1.674	2.378	
28	II	A	c	0.816	0.456	0.642		0.815	0.455	0.640	
29	II	B	c	1.173	0.656	0.929		1.169	0.654	0.926	
30	II	C	c	1.727	0.966	1.368		1.722	0.963	1.362	
31	III	A	c	0.640	0.358	0.506		0.637	0.356	0.504	
32	III	B	c	0.909	0.509	0.720		0.906	0.506	0.718	
33	III	C	c	1.315	0.736	1.041		1.311	0.733	1.039	
34	IV	A	c	0.365	0.205	0.289		0.363	0.204	0.286	
35	IV	B	c	0.505	0.283	0.400		0.502	0.280	0.398	

Table 3 (Continued)

No.	Slump	h/d	Group	Volume x 10^7 km^3	Thickness (km) 1	2	3	Adjusted Volume x 10^7 km^3	Adjusted Thickness (km) 1	2	3
36	IV	C	c	0.701	0.392	0.555		0.698	0.390	0.553	
37	I	A	d	1.463	0.816	1.159					
38	I	B	d	2.209	1.236	1.750					
39	I	C	d	3.488	1.952	2.762					
40	II	A	d	0.881	0.493	0.680					
41	II	B	d	1.297	0.726	1.027					
42	II	C	d	1.977	1.106	1.423					
43	III	A	d	0.683	0.382	0.541					
44	III	B	d	0.991	0.554	0.785					
45	III	C	d	1.480	0.828	1.172					
46	IV	A	d	0.375	0.210	0.297					
47	IV	B	d	0.528	0.295	0.418					

Table 3 (Continued)

No.	Slump	h/d	Group	Volume x 10^7 km^3	Thickness (km) 1	2	3	Adjusted Volume x 10^7 km^3	Adjusted Thickness (km) 1	2	3
48	IV	C	d	0.753	0.421	0.597					
49	I	A	e	1.401	0.784	1.110					
50	I	B	e	2.058	1.151	1.630					
51	I	C	e	3.130	1.751	2.479					
52	II	A	e	0.849	0.275	0.673					
53	II	B	e	1.221	0.683	0.967					
54	II	C	e	1.798	1.045	1.424					
55	III	A	e	0.666	0.373	0.528					
56	III	B	e	0.947	0.529	0.750					
57	III	C	e	1.369	0.766	1.084					
58	IV	A	e	0.380	0.212	0.301					
59	IV	B	e	0.526	0.294	0.417					

Table 3 (Continued)

No.	Slump	h/d	Group	Volume x 10^7 km^3	Thickness (km) 1	2	3	Adjusted Volume x 10^7 km^3	Adjusted Thickness (km) 1	2	3
60	IV	C	e	0.730	0.408	0.578					
61	I	A	f	0.127	0.072		0.194				
62	I	B	f	0.186	0.104		0.286				
63	I	C	f	0.284	0.159		0.436				
64	II	A	f	0.076	0.043		0.117				
65	II	B	f	0.110	0.062		0.169				
66	II	C	f	0.163	0.091		0.250				
67	III	A	f	0.060	0.034		0.092				
68	III	B	f	0.085	0.048		0.131				
69	III	C	f	0.123	0.069		0.190				
70	IV	A	f	0.033	0.019		0.051				
71	IV	B	f	0.047	0.026		0.072				
72	IV	C	f	0.065	0.037		1.000				

Table 4

Thickness of Ejecta in Selected Region of Southern Highlands

Slump	h/d	Class-Age	Volume x 10^6 km^3	Thickness (km) (Vol. ÷ 1.014 x 10^6)
I	A	a	1.935	1.908
I	B	a	2.836	2.795
I	C	a	4.296	4.240
II	A	a	1.175	1.158
II	B	a	1.686	1.661
II	C	a	2.472	2.438
III	A	a	0.936	0.924
III	B	a	1.311	1.292
III	C	a	1.886	1.860
IV	A	a	0.531	0.524
IV	B	a	0.734	0.724
IV	C	a	1.013	1.000

Table 5

Volume-Thickness Calculations for Circular Basins

	Name of Basin	Diameter (km)	h/d*	Volume for Slump Condition: ($\times 10^6$ km^3) I	III
**1.	Imbrium	670	0.038	7.70	2.25
**2.	Orientale (÷ 1/3)	390	0.060	1.82/3 = 0.61	0.61/3 = 0.20
**3.	Crisium	450	0.054	2.70	0.89
**4.	Humorum	420	0.057	2.25	0.75
**5.	Nectaris	400	0.058	2.00	0.65
6.	Near Schiller	180	0.090	0.21	0.09
**7.	Serenitatis	310	0.068	1.00	0.35
**8.	Humboldtianum	300	0.070	0.90	0.32
**9.	Smythi	370	0.062	1.60	0.54
10.	Fecunditatis	240	0.079	0.50	0.19
11.	W. Tranquillitatis	280	0.073	0.75	0.27
12.	E. Tranquillitatis	240	0.079	0.50	0.19
13.	Nubium	360	0.062	1.50	0.50
14.	Australe (÷ 1/2)	460	0.053	2.90/2 = 1.45	0.92/2 = 0.46
15.	Marginis	150	0.098	0.13	0.05
16.	Vaporum	200	0.076	0.30	0.12
17.	Sinus Iridum	260	0.076	0.62	0.23

Table 5 (Continued)

Name of Basin	Diameter (km)	h/d*	Volume for Slump Condition: ($\times 10^6$ km^3) I	III
18. Sinus Aestium	200	0.086	0.30	0.12
19. SE Limb	290	0.071	0.83	0.30

*Value read from curve for h/d function = 0.30-0.05

**These basins are underlain by mascons.

Volumes:
(km^3)

All basins; Slump I	25.85×10^6	
All basins; Slump III		8.47×10^6
Mascons; Slump I	18.76×10^6	
Mascons; Slump III		5.95×10^6

Thickness:
($\div 19.13 \times 10^6$ km^2)

All basins; Slump I	1.340 km	
All basins; Slump III		0.433 km
Mascons; Slump I	0.981 km	
Mascons; Slump III		0.311 km

Table 6

Summary of Thicknesses from Best Estimate Cases

	I*	(Thickness in km)	II*
CASE 1. III A including all basins**			
A. Highlands*	0.911	A. Highlands*	1.045
B. Basins (all)	0.443	B. Basins (all)	0.443
C. Mare (< 31 km)	0.004	C. Mare (< 31 km)	0.004
	1.358		1.492
CASE 2. III A; mascon basins only			
A. Highlands	0.911	A. Highlands	1.045
B. Mascons only***	0.311	B. Mascons only***	0.311
C. Mare (<31 km)	0.004	C. Mare (<31 km)	0.004
	1.226		1.360
CASE 3. III A for craters; no basin slump			
A. Highlands	0.911	A. Highlands	1.045
B. Basins (all)	1.340	B. Basins (all)	1.340
C. Mare (<31 km)	0.004	C. Mare (<31 km)	0.004
	2.255		2.389
CASE 4. III A for craters; no mascon slump			
A. Highlands	0.911	A. Highlands	1.045
B. Mascons only	0.981	B. Mascons only	0.981
C. Mare (<31 km)	0.004	C. Mare (<31 km)	0.004
	1.896		2.030

Table 6 (Continued)

*Highlands I includes all craters within a selected region in the south-central cratered province (centered on the crater Abenezra) covering a total area of 1.014×10^6 km^2; Highlands II includes all craters in age groups 1-3 larger than 15km diameter, all craters in ages 4-5 for all sizes, in classes C, aCM covering the entire exposed terrae of the front side of the Moon in an area of 12.62×10^6 km^2.

**Roman numeral-letter symbols (e.g., III A) refer to depth-diameter and slump functions defined in point 3 of Table 2.

***All basins include those listed by Hartmann and Kuiper (1962); mascons only refers to the following basins: Imbrium, Orientale, Crisium, Humorum, Nectaris, Serenitatus, Humboldtanium, and Smythi.

Table 7

Summary of Thicknesses for Special Cases

		(In km.)
CASE 1. Maximum Estimated Thickness:		
A. All C, aCM, pCM craters, groups d & e, no adjustments; I C		5.241
B. All basins; I C		2.740
C. pM; I C		0.024
	Sum:	8.005
CASE 2. Minimum Estimated Thickness:		
A. All C, aCM, pCM craters, excluding those less than 15 km wide; IV A		0.595
B. Mascons only; IV A		0.147
C. pM; IV A		0.002
	Sum:	0.744
CASE 3. Calculation of thickness of ejecta from pM (post mare) cratering of maria in which all ejecta remains entirely within the mare areas (6.55×10^6 km^2)		
A. Maximum thickness from all craters; I C		65.1 meters
B. Minimum thickness, fall craters; IV A		11.5
C. All craters; III A		17.8
D. All craters less than 50 km wide; III A		10.4

Table 7 (Continued)

E.	All craters less than 30 km wide; III A	6.2
F.	All craters less than 10 km wide; III A	1.8 meters

Table 8

Analysis of Impact Basin Underlying Mare Imbrium

1. Original diameter of basin of excavation = 670 km.
2. Depth of excavation (for h/d = 0.038 from function A) = 25.5 km.
3. Volume of excavation: A. No slump (I) = 7.70×10^6 km^3

   B. 20% slump (II) = 2.25×10^6 km^3
4. Initial rim height (no slump case) = 1/100 d = 6.7 km; Present rim probably lower (see step 7).
5. Total relief (from rim top to center of excavated basin surface) at time of formation: 25.5 + 6.7 = 32.2 km.
6. Present mare floor is, on average, 5.1 km below the Apennines (middle ring): about 1 km of ejecta may lie on the Apennine rim, so relief of inner ring is probably higher - select 6.0 km above mare surface.
7. However, original inner rim has all but disappeared: Assume it is just covered by mare material: Total relief between lowered rim and center of excavated basin surface becomes 32.2 - 6.0 = 26.6 km.
8. Assume backfill of basin of excavation (by slumping, fallback, throwout from other craters, highlands mass wasting, mascon-related adjustments) prior to emplacement of lavas:

   A. For backfill = 1/2 total original relief: 1/2 x 32.2 = 16.1 km (for this, less than 10% enlargement of diameter by slumping is needed)

Table 8 (Continued)

B. For backfill = 2/3 total relief: 2/3 x 32.2 = 21.5 km

C. For backfill = 3/4 total relief: 3/4 x 32.2 = 24.1 km (slumping enlarges diameter by more than 10%)

9. Maximum depth of lava infill (assume above top of backfill rubble) for each case in 8, on basis of present top of mare being 26.2 km above original base of excavation:

   A. 26.2 - 16.1 = 10.1 km of lava

   B. 26.2 - 21.5 = 4.7 km of lava

   C. 26.2 - 24.1 = 2.1 km of lava

10. For an ejecta blanket deposited between r (radius of basin of excavation extending to original rim) of 335 km and 4r (south of Fra Mauro crater), containing essentially all the volume of excavation (no slump), thickness of ejecta deposits next to rim, using a triangular wedge cross-section model, would be about 2 km; some ejecta may become involved in backfilling the basin of excavation.

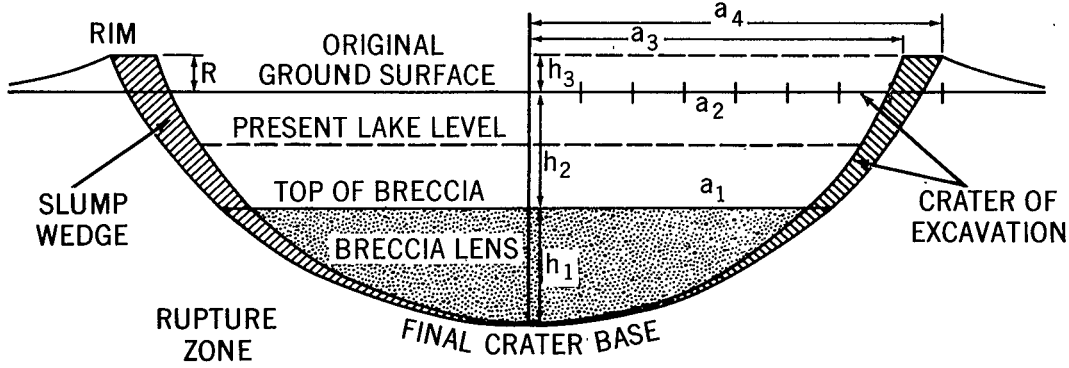

$$VOL = \frac{\pi}{6} h (h^2 + 3a^2)$$

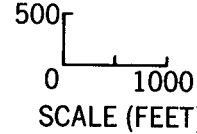

Figure 1. A generalized cross-section of a simple impact crater, adapted from a study of the West Hawk Lake structure in Canada (Short, 1970a). The outline of the initial crater of excavation is indicated by arrows. This crater has a diameter of a_2 and a depth of excavation = $h_1 + h_2$. Slumping increases the rim diameter a_3 to a final (observed) value of a_4, with the apparent limits of excavation now indicated by the final crater base outline. The depth to the apparent crater is $h_2 + h_3$ and to the true crater is $h_1 + h_2 + h_3$. The values a_2 and $h_1 + h_2$ are used in calculating the volume of the initial crater of excavation, from which all ejecta is assumed to come.

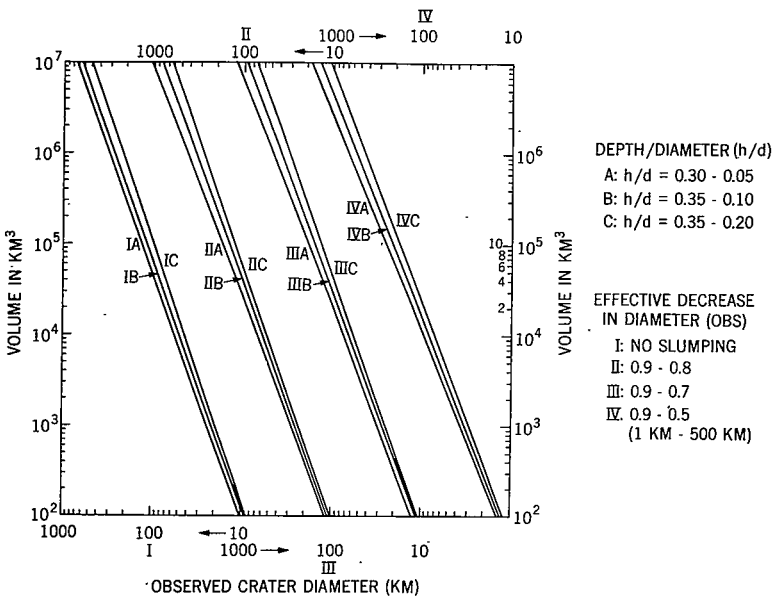

Figure 2. A series of computer-derived plots, on log-log scale, relating the observed crater diameter (a_4) to the volume of the initial crater of excavation. Twelve combinations of depth/diameter and slumping changes (see legend) were used to determine volumes of initial craters of excavation over the diameter range of 10-1000 km. The abscissa scale appropriate to each slumping condition is indicated by Roman numerals (on top and bottom). The observed crater diameter is used as an index but volumes are calculated on the basis of the decreased diameter obtained from each pertinent slumping function.

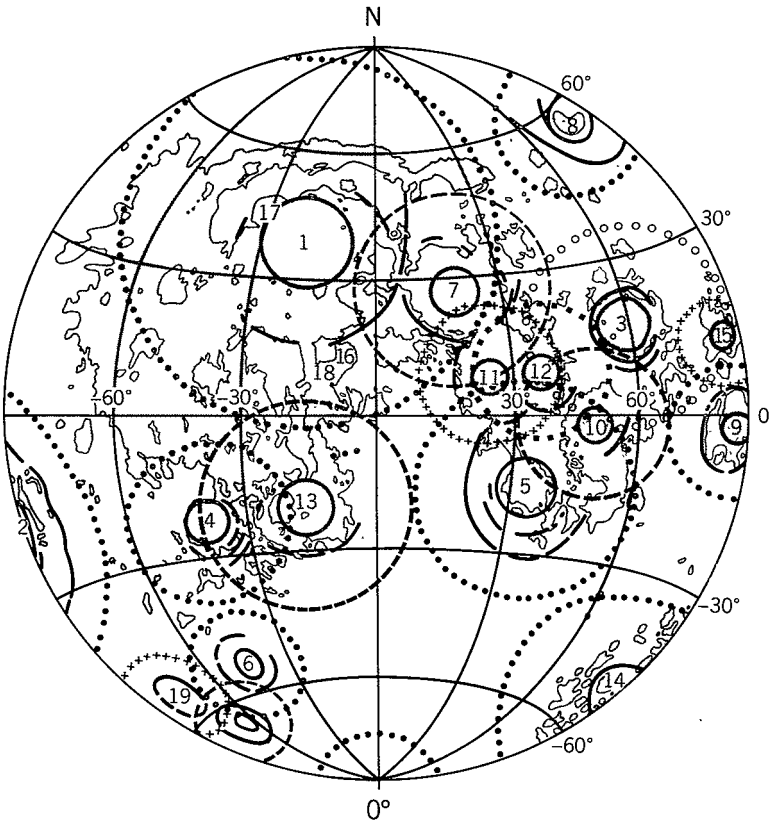

Figure 3. A map showing the distribution, in Lambert equal-area projection, of maria (shaded), large circular basins, and outer limits of associated ejecta blankets visible on the front side of the Moon (adapted from Stewart-Alexander and Howard, 1970). The circles outline the approximate limits of the inner rings of the indicated basins of excavation; in some cases, one or more outer rings are also located. The dots, squares, and crosses mark the positions at 3.5r (r = radius of inner ring) of the assumed edges of ejecta emanating from the basins occupying the circle centers. The basins are identified according to the number sequence given in Table 5.

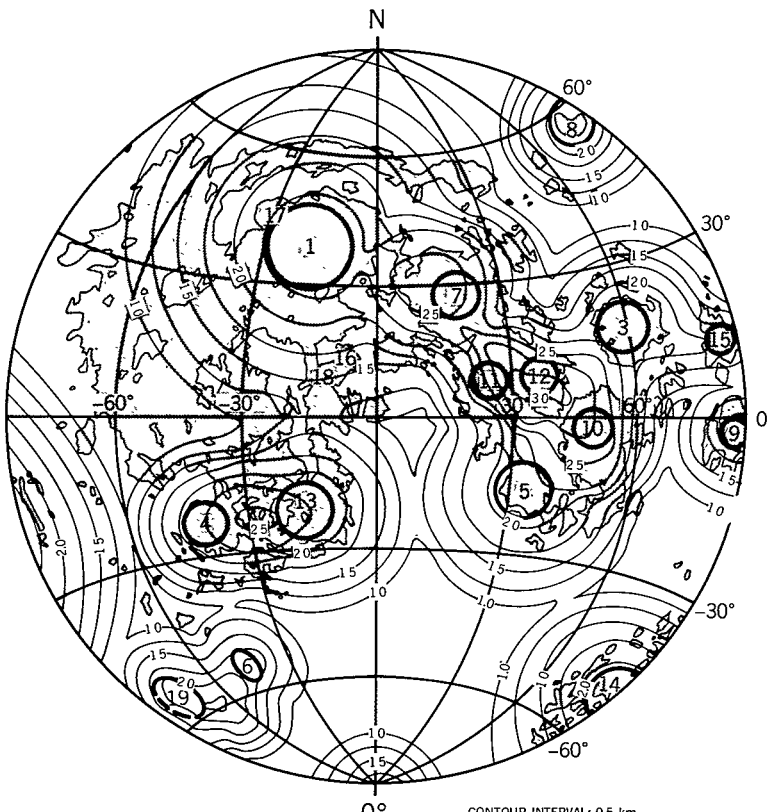

Figure 4. An isopach map, on the same base as Figure 3, of the distribution of ejecta blanket thicknesses on the front face of the Moon. The method by which thicknesses are calculated is discussed in the text. A minimum average thickness of 1 km is chosen for those areas, such as west (to the left) of Oceanus Procellarum and in the southern Highlands, which have not received deposits from the indicated basins of excavation.

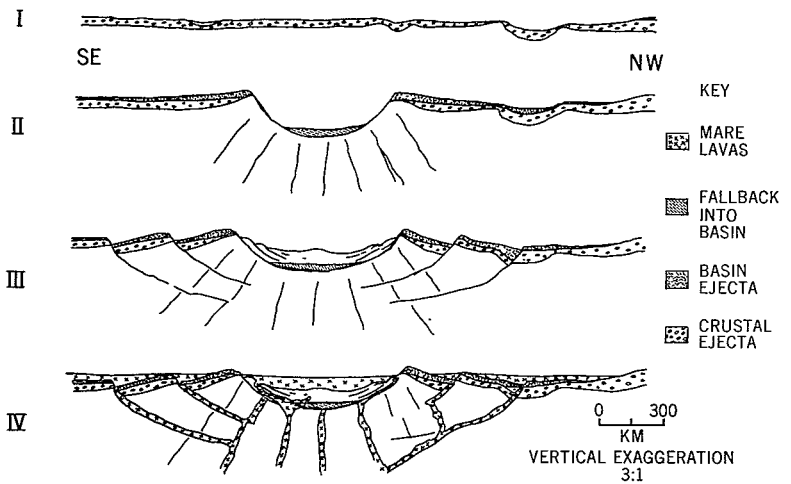

Figure 5. The inferred sequence of events (generalized) which produced the major features observed in the Mare Imbrium region of the Moon (based in part on Figure 1 in Hartmann and Kuiper, 1962). I. Formation of a continuous blanket of ejecta, about 1 km thick, derived from an intense, pre-basin episode of cratering over the entire lunar crust (composed possibly of anorthosite); II. Essentially instantaneous development of a basin of excavation, about 670 km wide and 25 km deep (see Table 7) by impact of a large meteorite or comet on to area now overlain by Mare Imbrium lavas. Most basin material is ejected on to surrounding crustal ejecta deposits, forming a new ejecta blanket as much as 1.5 to 2 km thick near the initial crater lip. A small fraction of the ejecta returns immediately to the basin as fallback. III. Formation of a series of roughly circular rings (3 or more) around the basin by a process similar to gravity sliding. The basin itself is expanded and partly infilled by slumping of its unstable walls. The entire time span over which the ringed valleys and scarps and the slump terraces were produced may have been only minutes to days. IV. Invasion, along the deep, impact-produced fractures that are presumed to penetrate into the sub-crust, of titaniferous basaltic lavas that fill both the central basin and most of the surrounding ringed valleys, leaving here and there some of the scarps still visible in this region.